ORGANIC LETTERS

2011
Vol. 13, No. 6
1498–1501

Coumarin-Based Thiol Chemosensor: Synthesis, Turn-On Mechanism, and Its Biological Application

Hyo Sung Jung,[†] Kyoung Chul Ko,[‡] Gun-Hee Kim,[§] Ah-Rah Lee,[§] Yun-Cheol Na,[∥] Chulhun Kang,[*,§] Jin Yong Lee,[*,‡] and Jong Seung Kim[*,†]

Department of Chemistry, Korea University, Seoul, 136-704, Korea, Department of Chemistry, Sungkyunkwan University, Suwon 440-746, Korea, The School of East-West Medical Science, Kyung Hee University, Yongin 446-701, Korea, and Seoul Center, Korea Basic Science Institute, Seoul 136-713, Korea

kangch@khu.ac.kr; jinylee@skku.edu; jongskim@korea.ac.kr

Received January 21, 2011

ABSTRACT

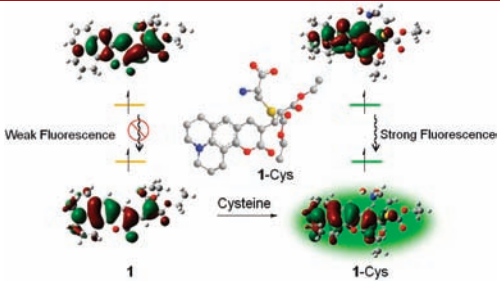

A new chemodosimetric probe (1) is reported that selectively detects thiols over other relevant biological species by the turning on of its fluorescence through a Michael type reaction. The fluorogenic process upon its reaction was revealed to be mediated by intramolecular charge transfer, as confirmed by time-dependent density functional theory calculations. The application of probe 1 to cells is also examined by confocal microscopy, and its cysteine preference was observed by an ex vivo LC-MS analysis of the cellular metabolite.

Thiols play important roles in the cellular antioxidant defense system.[1] Thiol groups play crucial roles in maintaining biological redox homeostasis through the equilibrium established between reduced free thiols (RSH) and oxidized disulfides (RSSR).[2] Moreover, their abnormal levels are known to be associated with human diseases such as slow growth, liver damage, skin lesions, Alzheimer's disease, cardiovascular disease, and coronary heart disease.[3]

Fluorescent probes possess innate advantages over other types of probes including their high sensitivity, specificity, simplicity of implementation, and ability to allow real-time monitoring due to their fast response times.[4] Accordingly, considerable effort has been made to develop fluorescent probes,[5] particularly for the detection of thiol species.[6−12] However, the practical utility of most of these probes has

[†] Korea University.
[‡] Sungkyunkwan University.
[§] Kyung Hee University.
[∥] Korea Basic Science Institute.

(1) (a) Chen, X.; Zhou, Y.; Peng, X.; Yoon, J. *Chem. Soc. Rev.* **2010**, *39*, 2120–2135. (b) Fersht, A., Ed. *Enzyme Structure and Mechanism*, 2nd ed.; Freeman, Co.: New York, 1984; pp 2−4.

(2) (a) Meister, A. *Methods Enzymol.* **1995**, *251*, 3–7. (b) Finkelstein, J. D.; Martin, J. J. *Int. J. Biochem. Cell Biol.* **2000**, *32*, 385–389. (c) Deneke, S. M. *Curr. Top. Cell Regul.* **2000**, *36*, 151–180.

(3) (a) Townsend, D. M.; Tew, K. D.; Tapiero, H. *Biomed. Pharmacother.* **2003**, *57*, 145–155. (b) Shahrokhian, S. *Anal. Chem.* **2001**, *73*, 5972–5978. (c) Carmel, R., Jacobsen, D. W., Eds. *Homocysteine in Health and Disease*; Cambridge University Press: Cambridge, U.K., 2001.

(4) (a) Kim, H. N.; Lee, M. H.; Kim, H. J.; Kim, J. S.; Yoon, J. *Chem. Soc. Rev.* **2008**, *37*, 1465–1472. (b) Kim, J. S.; Quang, D. T. *Chem. Rev.* **2007**, *107*, 3780–3799. (c) Quang, D. T.; Kim, J. S. *Chem. Rev.* **2010**, *110*, 6280–6301.

(5) (a) Bozdemir, O. A.; Guliyev, R.; Buyukcakir, O.; Selcuk, S.; Kolemen, S.; Gulseren, G.; Nalbantoglu, T.; Boyaci, H.; Akkaya, E. U. *J. Am. Chem. Soc.* **2010**, *132*, 8029–8036. (b) Liu, B.; Tian, H. *Chem. Commun.* **2005**, 3156–3158. (c) Kim, S. K.; Lee, S. H.; Lee, J. Y.; Lee, J. Y.; Bartsch, R. A.; Kim, J. S. *J. Am. Chem. Soc.* **2004**, *126*, 16499–16506.

(6) (a) Chen, X.; Ko, S.-K.; Kim, M. J.; Shin, I.; Yoon, J. *Chem. Commun* **2010**, *46*, 2751–2753. (b) Lee, K. S.; Kim, T. K.; Lee, J. H.; Kim, H. J.; Hong, J. I. *Chem. Commun.* **2008**, 6173–6175. (c) Yi, L.; Li, H.; Sun, L.; Liu, L.; Zhang, C.; Xi, Z. *Angew. Chem., Int. Ed.* **2009**, *48*, 4034–4037. (d) Hong, V.; Kislukhin, A. A.; Finn, M. G. *J. Am. Chem. Soc.* **2009**, *131*, 9986–9994. (e) Shiu, H.-Y.; Chong, H.-C.; Leung, Y.-C.; Wong, M.-K.; Che, C.-M. *Chem.−Eur. J.* **2010**, *16*, 3308–3313. (f) Sreejith, S.; Divya, K. P.; Ajayaghosh, A. *Angew. Chem., Int. Ed.* **2008**, *47*, 7883–7887.

10.1021/ol2001864
Published on Web 02/16/2011

been thwarted by their cross-sensitivities toward other biological analytes, narrow pH span,[7] and slow response[8] under physiological conditions. Therefore, it remains a challenging task to develop highly selective and efficient fluorescent probes for the detection of thiols. Recently, Lin et al. reported a ketocoumarin-based thiol detection probe featuring the 1,4-addition reaction of thiols to α,β-unsaturated ketones based on intramolecular charge transfer (ICT).[9] Li et al.[10] and Wu et al.[11] reported results regarding cysteine (Cys) selective fluorescent chemosensors.

Herein, the design and synthesis of a new fluorogenic probe (**1**) that emits fluorescence through its reaction with thiols, showing a preference for Cys, are reported. Upon its reaction with Cys, the representative thiol in this study, the fluorogenic process was revealed to be mediated by ICT, as confirmed by the time-dependent density functional theory (TDDFT) calculation performed in this study.

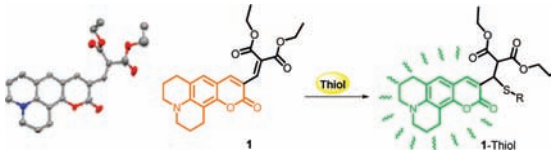

Figure 1. X-ray crystal structure of **1** and its fluorescent turn-on function for thiols. All hydrogen atoms are omitted for clarity. The thermal ellipsoids are shown at the 50% probability level.

Probe **1** was synthesized by the condensation of coumarinaldehyde and diethyl malonate, as shown in Scheme S1, and its structural identification was confirmed by ^{1}H NMR, ^{13}C NMR, and FAB-MS spectroscopy (Figures S20, S23, and S24). As shown in Figure 1, Cys can react with the β-carbon of α,β-unsaturated diesters *via* a Michael type addition reaction to generate the **1**-Cys adduct. The detailed NMR spectra, including 2D HSQC (Heteronuclear Single Quantum Coherence), for the **1** and **1**-Cys adducts, are depicted in Figures S1 and S2, respectively. The signals of the H_1-H_3 protons of **1** appear at 7.65, 7.75, and 6.99 ppm, respectively. Then, the ^{1}H NMR spectrum of **1** in a solution of D_2O/CD_3CN (3:7) was monitored upon the addition of Cys at room temperature. As the vinylic proton (H_1) at 7.65 ppm disappeared, two new peaks appeared at 4.35 and 4.27 ppm, obviously caused by the formation of the **1**-Cys adduct (Figure S2). The FAB-MS spectrometry analysis of probe **1** treated with Cys in aqueous solution (10 mM PBS buffer, pH 7.4, 10% DMSO) also confirms the formation of the **1**-Cys adduct. The mass spectrum displayed a peak at m/z 533.41 $[M+H]^+$ (Figure S21). This Michael type reaction was further confirmed by the reaction of probe **1** with 2-mercaptoethanol, whose detailed ^{1}H NMR and FAB-MS data are presented in Figures S3 and S22, respectively.

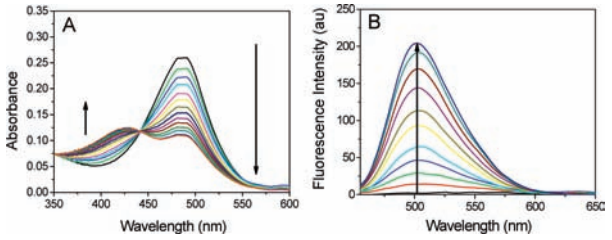

Figure 2. (A) UV−vis and (B) fluorescence spectra of **1** (5.0 μM) in aqueous solution (10 mM PBS buffer, pH 7.4, 10% DMSO) upon addition of various concentrations of Cys (0−100 equiv). Excitation at 440 nm (slit = 1.5/3).

During the 1,4-addition reaction to **1**, the conjugation of the coumarin ring system to the α,β-unsaturated carbonyl group was broken, resulting in changes in both the UV/vis and fluorescence spectra. Indeed, as shown in Figure 2, the addition of Cys to **1** induced a 62 nm hypsochromic shift of the absorption maximum at λ_{ab} = 426 nm, resulting in a perceived color change from dark orange to green, while the fluorescence maximum at λ_{em} = 502 was enhanced *ca.* 107-fold (Φ_f = 0.3268; see Table S1). Homocysteine and glutathione (Hcy and GSH) demonstrated similar characteristics. In contrast, probe **1** exhibited nonfluorescence (Φ_f = 0.0056; see Table S1) due to the ICT from the fluorophore (coumarin) to the nearby conjugated diester (*vide infra*).

To investigate the mechanism of the fluorescence enhancement during the formation of the **1**-thiol adduct, DFT calculations were carried out for the **1**-Cys adduct with 6-31G* basis sets using a suite of Gaussian 03 programs.[12] The optimized structures of **1** and **1**-Cys are shown in Figure 3. Probe **1** has a conjugated bridge (−C═C−) between the coumarin and diester groups, while **1**-Cys has a saturated bridge (−C−C−). The calculated structure of **1** was in good agreement with the experimental crystal structures shown in Figure 1. It is of note that one of the two ester groups of **1** is located in the same plane as the coumarin ring system, unlike the corresponding ester groups in **1**-Cys. This structural difference leads to the strong, anticipated ICT process in **1**

(7) Tanaka, F.; Mase, N.; Barbas, C. F., II. *Chem. Commun.* **2004**, 1762–1763.
(8) Pires, M. M.; Chmielewski, J. *Org. Lett.* **2008**, *10*, 837–840.
(9) Lin, W.; Yuan, L.; Cao, Z.; Feng, Y.; Long, L. *Chem.−Eur. J.* **2009**, *15*, 5096–5103.
(10) Li, H.; Fan, J.; Wang, J.; Tian, M.; Du, J.; Sun, S.; Sunb, P.; Peng, X. *Chem. Commun.* **2009**, 5904–5906.
(11) Wu, H.; Huang, C.; Cheng, T.; Tseng, W. *Talanta* **2008**, *76*, 347–352.
(12) Frisch, M. J.; Trucks, G. W.; Schlegel, H. B.; Scuseria, G. E.; Robb, M. A.; Cheeseman, J. R.; Montgomery, J. A., Jr.; Vreven, T.; Kudin, K. N.; Burant, J. C.; Millam, J. M.; Iyengar, S. S.; Tomasi, J.; Barone, V.; Mennucci, B.; Cossi, M.; Scalmani, G.; Rega, N.; Petersson, G. A.; Nakatsuji, H.; Hada, M.; Ehara, M.; Toyota, K.; Fukuda, R.; Hasegawa, J.; Ishida, M.; Nakajima, T.; Honda, Y.; Kitao, O.; Nakai, H.; Klene, M.; Li, X.; Knox, J. E.; Hratchian, H. P.; Cross, J. B.; Bakken, V.; Adamo, C.; Jaramillo, J.; Gomperts, R.; Stratmann, R. E.; Yazyev, O.; Austin, A. J.; Cammi, R.; Pomelli, C.; Ochterski, J. W.; Ayala, P. Y.; Morokuma, K.; Voth, G. A.; Salvador, P.; Dannenberg, J. J.; Zakrzewski, V. G.; Dapprich, S.; Daniels, A. D.; Strain, M. C.; Farkas, O.; Malick, D. K.; Rabuck, A. D.; Raghavachari, K.; Foresman, J. B.; Ortiz, J. V.; Cui, Q.; Baboul, A. G.; Clifford, S.; Cioslowski, J.; Stefanov, B. B.; Liu, G.; Liashenko, A.; Piskorz, P.; Komaromi, I.; Martin, R. L.; Fox, D. J.; Keith, T.; Al-Laham, M. A.; Peng, C. Y.; Nanayakkara, A.; Challacombe, M.; Gill, P. M. W.; Johnson, B.; Chen, W.; Wong, M. W.; Gonzalez, C.; Pople, J. A. *Gaussian 03*, revision C02; Gaussian Inc.: Pittsburgh, PA, 2004.

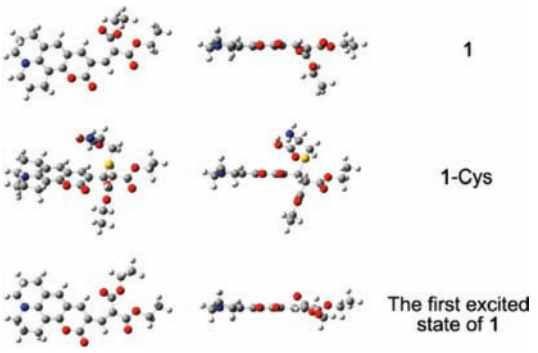

Figure 3. Optimized structures of **1**, **1**-Cys, and the first excited state of **1**.

and weakened ICT in **1**-Cys. In addition, as shown in Figure 3, the optimized structure for the first excited state of **1** shows that both ester groups have a greater planar geometry with the coumarin plane than that of **1**-Cys, which inhibits the fluorescence emission from **1**.

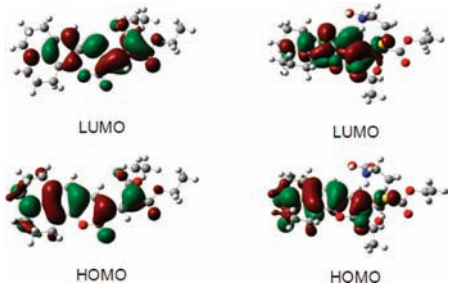

Figure 4. Calculated HOMOs and LUMOs of **1** (left column) and **1**-Cys (right column).

Detailed information regarding the marked fluorescence enhancement upon the formation of **1**-Cys can be obtained from TDDFT calculations. The calculated excitation wavelength of **1**-Cys was 355 nm, which was blue-shifted by 56 nm from that of **1** (411 nm). The magnitude of the calculated blue shift is in agreement with the experimentally observed one (62 nm). The HOMOs and LUMOs of **1** and **1**-Cys are shown in Figure 4. The HOMO→LUMO transition contributed 100% and 97.4% to the excitation of **1** and **1**-Cys, respectively. Thus, the electron density distribution is confined to the LUMO after its excitation. From the LUMOs, it is clear that the ICT takes place through a conjugated bridge between the coumarin and diester groups in **1**, while this is obviously prohibited in **1**-Cys due to the nonconjugated bridge. This result supports the hypothesis that the strong fluorescence emissions from the **1**-Cys adduct are due to its weakened ICT process relative to that in **1**.

A comparison of the reactivity of **1** toward Cys, Hcy, or GSH was performed by monitoring the fluorescence changes of the reaction mixture in aqueous solution

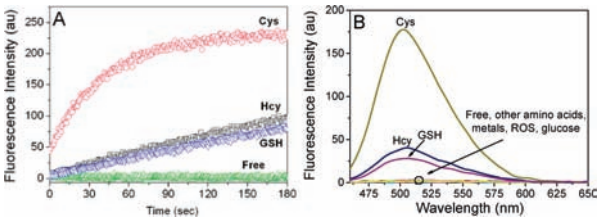

Figure 5. (A) Time course of the fluorescence response of probe **1** (5.0 μM) in aqueous solution (10 mM PBS buffer, pH 7.4, 10% DMSO), regarding the presence of 100 equiv of Cys, Hcy, or GSH, with an excitation at 440 nm. The fluorescence intensity was recorded near 502 nm at room temperature. (B) Fluorescence spectra of **1** (5.0 μM) in aqueous solution (10 mM PBS buffer, pH 7.4, 10% DMSO) in the presence of various amino acids, metals, ROS, and glucose (100 equiv, respectively) at an excitation wavelength of 440 nm after 1 min.

(10 mM PBS buffer, pH 7.4, 10% DMSO), and the results are depicted in Figure 5A. The time course of the fluorescence intensity in a mixture of Cys and **1** seems to follow a single exponential function. Hcy and GSH also showed increases in their fluorescence intensity, but at much lower rates. Indeed, the kinetic analysis based on a single exponential decay model showed that **1** reacts with Cys 13- and 21-fold faster than with Hcy and GSH, respectively (Figure S5). This result leads to the conclusion that **1** has a preference for Cys over other biologically important thiols. We found that the fluorescence intensity is proportional to the amount of Cys added at a submicromolar level, with a coefficient of $R = 0.99557$ (Figure S9) and a detection limit of 30 nM (Figure S10). In addition, as indicated in Figure S11, the fluorescence change of **1** with Cys is independent of the pH in the range of 6 to 11. These results again imply that **1** may prefer Cys over other thiols in biological systems.

To further investigate the preferences of probe **1** toward different thiols in biological media, the fluorescence spectral changes were examined during the reaction of **1** with various biologically relevant analytes in aqueous solution (10 mM PBS buffer, pH 7.4, 10% DMSO). Probe **1** showed a marked enhancement in its fluorescence intensity upon its selective reaction with thiol containing amino acids over other amino acids (Ala, Arg, Asn, Asp, Gln, Gluc, Glu, Gly, His, Ile, Leu, Lys, Met, Phe, Pro, Ser, Tau, Thr, Trp, Tyr, Val), biologically common metal ions (K^+, Ca^{2+}, Mg^{2+}, Na^+, Zn^{2+}, Fe^{2+}, Fe^{3+}), oxidoreducing agents (H_2O_2, NADH), and glucose (Figures 5B and S13). In addition, competitive experiments for the reaction of **1** with Cys in the presence of other biologically relevant analytes revealed no significant influence of them on the Cys sensing (Figures S12 and S13).

Regarding the Cys preference of **1**, it is interesting to point out that the pK_a of Cys (8.30) is lower than that of Hcy (8.87) or GSH (9.20).[13] Thus, under the experimental

(13) Iciek, M.; Chwatko, G.; Lorenc-Koci, E.; Bald, E.; Wlodek, L. *Acta Biochim. Polonica* **2004**, *51*, 815–824.

conditions in this study (pH 7.4), the thiol of Cys is presumably changed to the thiolate which becomes a better nucleophile in Michael addition reactions. Therefore, it can be assumed that, at higher pH, this selectivity would disappear. In fact, the relative ratio of the fluorescence intensities of probe **1** with GSH to that with Cys was largely increased as the solution pH shifted to the basic side (Figure S14), supporting the hypothesis that the Cys selectivity of probe **1** may be partly due to the relatively lower pK_a value of Cys compared to that of the other thiols. However, this explanation may be applicable to many other thiol probes and not be unique to probe **1**. Another possible origin of this preference could be a steric effect, according to a report that the thiol group of Cys is sterically less hindered than those of Hcy and GSH.[9]

LC/MS spectroscopy was also employed to investigate the Cys preference over Hcy and GSH. In the copresence of Cys, Hcy, and GSH (100 equiv each), **1** preferably reacted with Cys to give **1**-Cys as the major peak in the ion monitoring chromatogram, whereas the peak intensities of **1**-Hcy and **1**-GSH were relatively small (Figure S18). These apparent differences might be caused by the different efficiencies of ionization. Under similar LC-MS conditions, a longer reaction time allows **1** to form significant amounts of the Cys adduct, Hcy, and GSH, and each corresponding adduct was reasonably detectable (Figure S17). These results imply that the differences in the peak intensities of the adducts in Figures S18 and S19 are not caused by the differences in their ionization efficiencies in the MS compartment in this instrument, but rather by their reactivity differences shown in Figure 5A.

With this more practical evidence of the preference of **1** toward Cys taken into account, the reaction of cellular metabolites with probe **1** was examined by LC-MS spectroscopy. To obtain the metabolites, the cytosolic cell extracts were treated by removing the macromolecules through acetone precipitation. After the reaction of **1** with the prepared metabolite mixture, LC-MS analysis was performed and parts of the resulting LC-MS profiles are shown in Figure S19. The major fluorescent adduct was apparently from **1**-Cys. The profiles in Figure S19 are similar to those in Figure S18. These results confirm that the major species detected by LC-MS analysis is the Cys-**1** adduct, although the most abundant thiol species within the cells may be GSH, suggesting that **1** may prefer Cys over other thiols in biological systems. A similar analysis of the cellular adducts from the cells treated with probe **1** would provide pivotal evidence for its Cys selectivity. However, this was not attempted, because the Cys preference of probe **1** is time-dependent and its reactions with the intracellular thiol species could not be stopped during preparation of the samples for analysis.

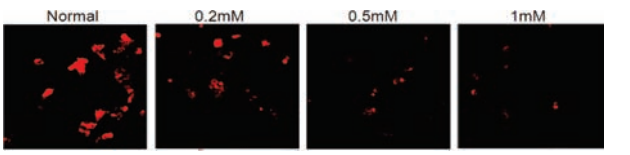

Figure 6. Confocal microscopic analysis of HepG2 cells treated with compound **1**. The images of the cells were obtained using excitation at 488 nm and a long-path (> 560 nm) emission filter. For the NEM-treated samples, before the media were finally replaced with PBS containing compound **1**, the cells were incubated with media containing NEM at various concentrations for 1 h at 37 °C.

In order to further demonstrate that probe **1** can detect intracellular thiols, confocal microscopy experiments were conducted. Figure 6 shows the fluorescence images of HepG2, a human hepatoma cell line, a selective thiol modifying reagent. The fluorescence intensity decreased upon the addition of NEM, inferring that the species containing thiol groups, such as Cys, Hcy, GSH, or the proteins in the cells are responsible for the fluorescence enhancement. The incubation of probe **1** with dialyzed cytosolic protein extract failed to show any intensity in the fluorescence spectroscopic experiments (data not shown).

In conclusion, the new coumarin-based chemodosimeter **1** effectively and selectively recognizes thiols based on a Michael type reaction, showing a preference for cysteine over other biological materials including homocysteine and glutathione. From the TDDFT calculations, it was determined that the fluorescence amplification of **1** upon its reaction with thiols is due to an ICT blocking event. The cysteine preference of **1** over homocysteine and glutathione was also proven by LC-MS spectroscopic methods using the metabolite from the HepG2 cell line. In the confocal microscopy study, **1** showed a marked fluorescence enhancement for cysteine over other thiol functionalized amino acids.

Acknowledgment. This work was supported by the CRI program (No. 2010-0000728) of the National Research Foundation of Korea (J.S.K.). The work at SKKU was supported by an NRF grant (No. 20100001630) funded by MEST and a Samsung Research Fund, Sungkyunkwan University, 2010.

Supporting Information Available. Text and figures giving details of the UV−vis, fluorescence spectral data, kinetic data, calculations, and characterization. This material is available free of charge via the Internet at http://pubs.acs.org.